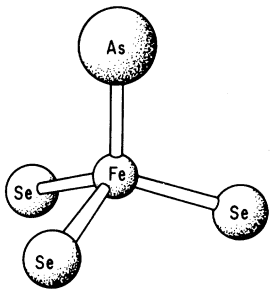

FIG. 5. Model of the center with Fe^{3+} substitutional for Zn^{2+} and As^{3-} substitutional for a nearest Se^{2-}.

$$\mathcal{H} = \beta \vec{H} \cdot \overleftrightarrow{g} \cdot \vec{S} + D[S_z^2 - \tfrac{1}{3}S(S+1)] + \tfrac{1}{6}a[S_\xi^4 + S_\eta^4 + S_\zeta^4 - \tfrac{1}{5}S(S+1)(3S^2+3S-1)] + \tfrac{1}{180}F[35S_z^4 - 30S(S+1)S_z^2 + 25S_z^2 - 6S(S+1) + 3S^2(S+1)^2] .$$

The ξ, η, ζ axes are parallel to the fourfold cubic axes. The connection between the parameters appearing in the two forms is given by

$$b_2^0 = \tfrac{1}{3}D, \quad b_4^0 = \tfrac{1}{180}(F-a), \quad b_4^3 = \tfrac{1}{9}(a/2) ,$$

where only the cubic contribution to b_4^3 has been considered.

†Research sponsored in part by the Air Force Office of Scientific Research, Contract No. F44620-67-C-0073.

[1]R. S. Title, B. L. Crowder, and J. W. Mayo, in *II-VI Semiconducting Compounds*, edited by D. G. Thomas (Benjamin, New York, 1967), p. 1367; J. Schneider, *ibid.*, p. 40; R. K. Watts and W. C. Holton, Phys. Rev. 173, 417 (1968); W. C. Holton, M. de Wit, R. K. Watts, T. L. Estle, and J. Schneider, J. Phys. Chem. Solids 30, 963 (1969).

[2]W. C. Holton, M. de Wit, T. L. Estle, B. Dischler, and J. Schneider, Phys. Rev. 169, 359 (1968).

[3]W. C. Holton, R. K. Watts, and R. D. Stinedurf, J. Crystal Growth 6, 97 (1969).

[4]W. C. Holton, A. R. Reinberg, R. K. Watts, and M. de Wit, J. Luminescence 1, 583 (1970).

[5]H. H. Wickman, M. P. Klein, D. A. Singleton, J. Chem. Phys. 42, 2113 (1965).

[6]J. E. Bennett, J. F. Gibson, and D. J. E. Ingram, Proc. Roy. Soc. (London) A240, 67 (1957).

[7]M. T. Hutchings, in *Solid State Physics*, edited by F. Seitz and D. Turnbull (Academic, New York, 1964), Vol. 16, p. 227.

[8]E. S. Kirkpatrick, K. A. Müller, and R. S. Rubins, Phys. Rev. 135, A86, (1964).

[9]H. Watanabe, J. Phys. Chem. Solids 25, 1471 (1964).

[10]H. Watanabe, in *II-VI Semiconducting Compounds*, edited by D. G. Thomas (Benjamin, New York, 1967), p. 1381.

[11]J. Schneider, S. R. Sircar, and A. Räuber, Z. Naturforsch. 18A, 980 (1963).

PHYSICAL REVIEW B VOLUME 2, NUMBER 5 1 SEPTEMBER 1970

Electronic Raman Spectrum and Crystal Field of the Terbium Ion in Terbium Aluminum Garnet*

J. A. Koningstein and G. Schaack†
Department of Chemistry, Carleton University, Ottawa, Ontario, Canada
(Received 29 September 1969)

Electronic Raman transitions of Tb^{3+} in $Tb_3Al_5O_{12}$ (garnet) within the $^7F_6$ ground-state components and to the excited states of the $^7F_5$ components have been observed. From the polarization properties of the Raman transitions, the symmetry of some of the states of the Tb^{3+} ions in this crystal has been determined. A Zeeman–Raman experiment has been performed. Relations between the observed components of the scattering tensors of cubic symmetry and the tensors for transitions of the ions in the orthorhombic site symmetry have been established. Based on these results, the justification of the cubic and tetragonal approximations of the crystal field in this compound is discussed.

I. INTRODUCTION

The study of transitions between electronic states of the $4f$ shell of rare-earth ions in solids by inelastic scattering of light is a relatively new branch of research.[1] The present available extensive knowledge of these states – that is, the energy of the states and the wave functions – has been the result of studies of electric and magnetic dipole transitions between these states.[2] However, the observations of Raman transitions of trivalent rare-earth ions in solids occurred, except in one case,[3] after the advent of the laser,[4] and the importance of this new technique with regard to extending the above-mentioned properties may lead to new developments in the application of crystal-field theory.[5] There are two reasons why these developments may take place. First, the Raman

operator is an even-parity operator and, thus, electronic Raman transitions between states of the same parity are formally allowed. This is in direct contrast to electric dipole transition between such states. Second, the Raman process is related to a tensor of second rank and the nonvanishing components of a particular transition are intricately related to the symmetry of the states which are involved in the scattering process.[6]

The selection rules, based on the symmetry of the crystal, differ for Raman transitions from those for electric dipole or magnetic dipole transitions. Usually, the number of transitions which is allowed in the Raman effect is larger than the number of transitions for photon absorption or emission by electric or magnetic dipoles. It may therefore be possible to reveal the positions of some electronic states which, up to now, have escaped spectroscopic observation because of selection rules for the conventional spectroscopic experiments. Especially for cubic crystals with isotropic optical properties and dipole transitions, no specific information on the orientation of these dipoles can be obtained. However, cubic crystals have anisotropic Raman scattering properties which permit identification of the symmetry of the states involved. In particular, this feature is of relevance to this paper as will be indicated below.

In the case of rare-earth ions in garnet crystals it is well known that the lanthanides occupy sites of orthorhombic symmetry. The proper symmetry is given by the point group D_2. The garnet crystals belong to the space group O_h^{10} and there are 24 rare-earth ions in the unit cell of rare-earth garnets.[7-10] These ions have identical environments but there are six different orientations of the D_2 axes of these sites with respect to the directions of the macroscopic axes of the cubic crystal. The symmetry labeling of the Stark levels in terms of the irreducible representations of the group D_2 is of no importance in the case of rare-earth ions with an odd number of $4f$ electrons. Here, only the Γ_5 representation of the double group D_2 is involved and the Raman scattering tensor between states of such symmetry resembles a tensor which is normally encountered if the states are labelled with species of a point group of very low symmetry.[10] For rare-earth ions with an even number of $4f$ electrons (non-Kramers ions) a labeling of the states in terms of four representations A, B_1, B_2, and B_3 of the point group D_2 should be made. The scattering tensor for transitions between states of such symmetry belongs also to these species, and labeling of the individual states can be accomplished. This is important if the results of crystal-field calculations are compared with the results of the Raman studies and it is here, where electronic Raman spectroscopy is advantageous by comparison to a similar situation, where only absorption or fluorescence measurements are employed to perform an analysis.

In this paper we discuss electronic Raman transitions of a single crystal of terbium aluminum garnet. From the Raman scattering tensors of some of the transitions, not only could the symmetry of crystal-field levels be determined, but also it was found that the symmetry of the crystal field at the site of the Tb^{3+} ions is approximately tetragonal.

II. EXPERIMENTAL

Raman spectra of an oriented single crystal of terbium aluminum garget – TbAlG – were excited with the 6328- and 5145-Å radiation of commercially available lasers. The single crystal was mounted in such a way that the direction of propagation of the laser beam was parallel to the c axes of the cubic crystal, while the direction of observation of the scattered light was made at an angle of 45° with either the a or b axis of the crystal. Raman lines were studied with shifts of up to 2400 cm^{-1} from the exciting lines with the temperature of the sample at 10, 80, and 300 °K. A double monochromator was employed to separate the Raman transitions and all spectra were photoelectrically recorded.

Raman studies with the sample exposed to a magnetic field were also carried out.[11] The position of the sample and the direction of the magnetic field are shown in Fig. 1. The temperature of the sample during the Zeeman experiments was 4.2 °K. Because of the fact that the incident exciting radiation and also the scattered light had to pass several Pyrex glass windows, the intensity of the Raman transitions was lowered by about one order of magnitude compared to the intensity of the spectra obtained with the crystal mounted on top of the cold finger of a He research Dewar. Although the strength of the magnetic field could be varied from 0 to 48 kG, the slit of the monochromator had to be opened, and spectra could only be recorded with an experimental slit width of ~5 cm^{-1}.

III. RAMAN SPECTRUM OF TbAlG

The experimental conditions under which the Raman spectra were studied have already been indicated in Sec. II. The experimental axes – that is, the laboratory axes – coincide apparently with the local D_2 axes of one of the sites for rare-earth ions in garnet crystals. Independently of the symmetry of the state in which the Raman transitions originate or the symmetry of the terminal state, all nonvanishing elements of the scattering tensor

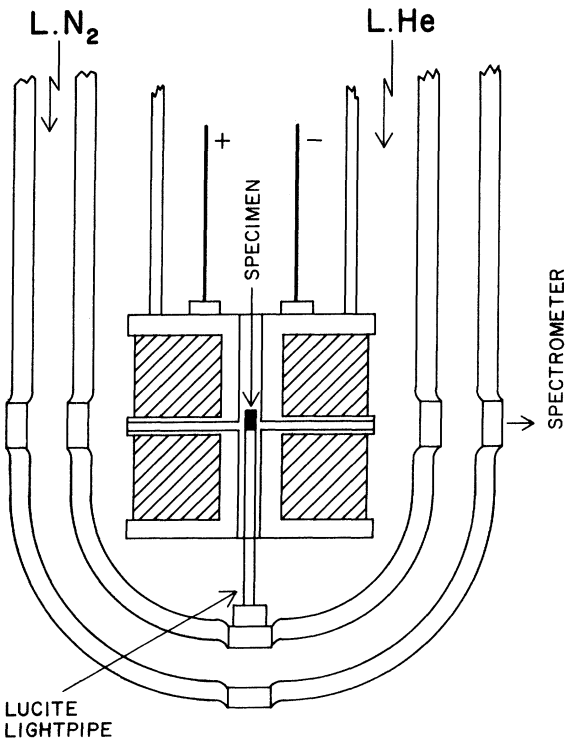

FIG. 1. Schematic of superconducting magnet for a Zeeman-Raman experiment. The laser beam enters through a hole in the bottom of the magnet and the scattered radiation is observed at 90°.

belong to the species A_{1g}, E_g, T_{2g}, and T_{1g} of the point group O_h. The latter species represent the antisymmetric part of the scattering tensor, i.e., $\alpha_{xy} - \alpha_{yx}$, etc. The relation between the scattering properties of the single rare-earth ions of site symmetry D_2 and the macroscopic tensors for the cubic crystal will be discussed in more detail in Sec. V. Group theory predicts that in this situation the irreducible representations of the point group D_2 and the subsequently induced representations of the group O_h are correlated in the normal way as shown in Table I. The scattering tensors which belong to these species are, however, not the tensors which pertain to the experimental situation. In fact, the appropriate tensors have to be adapted to the experimental situation[12] and these tensors are given in Table II. There does exist a unique way to study the tensors in this particular situation. The relative intensities of the Raman lines can be expressed as function an angle φ. This angle represents the rotation of the electric vector of the incident laser radiation with regard to the optical axis of the spectrometer, and $\varphi = 0$ if the vector is parallel to this optical axis. The various scattering tensors can thus be separated by a study of the intensity of Raman lines as a function of the angle φ. The equations given in Table III represent the dependence of the intensity of Raman lines. A part of the Raman spectrum of TbAlG as a function of the angle φ is shown in Fig. 2.

The assignment of the complete phonon spectrum has been made employing this technique and the reader is referred to an earlier publication for complete details.[12] The frequencies and assignment of the low-temperature Raman spectrum of the compound is given in Table IV, and a discussion of the electronic Raman transitions is offered in Sec. IV.

IV. ELECTRONIC RAMAN TRANSITIONS

The energy levels of the trivalent terbium ion are related to the (Xe)$4f^8$ electronic configuration. This configuration gives rise to a large number of LSJ manifolds and of interest to this work are the crystal-field levels of the $^7F_6$ and $^7F_5$ manifolds of TbAlG. Because of the fact that the symmetry of the field, which the Tb^{3+} ion experiences, is orthorhombic it is expected that the $(2J+1)$-fold degeneracy of the J manifolds is completely removed. The center of gravity of the $^7F_6$ manifold is about 2000 cm^{-1} above the ground state, and from the selection rules for the electronic Raman effect[13,14] it is concluded that transitions within the crystal-field components of the $^7F_6$ ground manifold and the $^7F_5 \rightarrow {}^7F_6$ intermanifold transitions are allowed.

Evidence of electronic Raman transitions of TbAlG have been reported in an earlier publication.[15] A knowledge of the phonon spectrum of this crystal is also important because the position of crystal-field levels of the $^7F_6$ manifold is in the range of the phonon modes of the crystal. This does not pertain to the intermanifold electronic Raman transitions; they occur with shifts of more than 2000 cm^{-1} and phonon modes of the garnet crystals do not exist in that range.[12] In Fig. 3 we show the Raman spectrum in that interval. The temperature of the sample was 80 °K and the spectrum was excited with the 5145-Å line of an argon-ion laser. Strong fluorescence was excited if the 4880-Å emission

TABLE I. Correlation of irreducible representations of site and factor group for rare-earth ions in garnet systems.

Species of D_2	Species of O_h[a]
A	$A_{1g} + E_g + T_{2g}$
B_1	$E_g + T_{1g}$
B_2	$T_{2g} + T_{1g}$
B_3	$T_{2g} + T_{1g}$

[a] Only the transformation properties of the Raman scattering tensor are given.

TABLE II. Scattering tensors for the experimental situation.

$$A_{1g}: \begin{pmatrix} a & 0 & 0 \\ 0 & a & 0 \\ 0 & 0 & a \end{pmatrix}$$

$$E_g: \sqrt{3}\begin{pmatrix} 0 & -b & 0 \\ -b & 0 & 0 \\ 0 & 0 & 0 \end{pmatrix}; \quad \begin{pmatrix} b & 0 & 0 \\ 0 & b & 0 \\ 0 & 0 & -2b \end{pmatrix}$$

$$T_{2g}: \frac{1}{\sqrt{2}}\begin{pmatrix} 0 & 0 & c \\ 0 & 0 & c \\ c & c & 0 \end{pmatrix}; \frac{1}{\sqrt{2}}\begin{pmatrix} 0 & 0 & c \\ 0 & 0 & -c \\ c & -c & 0 \end{pmatrix}; \begin{pmatrix} c & 0 & 0 \\ 0 & -c & 0 \\ 0 & 0 & 0 \end{pmatrix}$$

$$T_{1g}: \frac{1}{\sqrt{2}}\begin{pmatrix} 0 & 0 & d \\ 0 & 0 & d \\ -d & -d & 0 \end{pmatrix}; \frac{1}{\sqrt{2}}\begin{pmatrix} 0 & 0 & d \\ 0 & 0 & -d \\ -d & d & 0 \end{pmatrix}; \begin{pmatrix} 0 & d & 0 \\ -d & 0 & 0 \\ 0 & 0 & 0 \end{pmatrix}$$

impinged on the crystal because of resonance between the energy of the laser radiation and one of the $^5D_4$ manifold levels. Some of the Raman lines of Fig. 3 disappeared upon cooling the sample to 10 °K. From the position of these Raman lines the conclusion was drawn that low-lying electronic levels of TbAlG are situated at 75 and 86 cm^{-1} above the ground state. These levels must belong to Tb^{3+} ion because the occurrence of vibroelectronic Raman effects has been shown to have negligible intensity.[13] Some of the Raman lines of Fig. 3 show a shoulder on the low-energy side, and they are due to electronic transitions which originate in a level which is situated at only ~5 cm^{-1} above the ground state of TbAlG. The location of four of the possible 13 crystal-field components of the $^7F_6$ manifold could thus be determined from the Raman spectrum shown in Fig. 3. The position of levels of the $^7F_5$ manifold follows directly from the 10 °K Raman spectrum. Positions and symmetry of the Raman transitions are given in Table IV.

The part of the Raman spectrum of TbAlG with shifts < 900 cm^{-1} is shown in Fig. 4. Very strong Raman scattering occurs to two bands shifted by some 80 cm^{-1} from the exciting line. Phonon modes of the garnet crystal do not occur at that position and these transitions are therefore assigned to the above-discussed electronic levels of the terbium ion. The anti-Stokes components were also observed even at low temperature of the sample. A Zeeman-Raman study of these lines has been made and the results are shown in Fig. 5. Upon lowering of the temperature of the crystal it was noted that the Raman line centered at 81.5 cm^{-1} decreased in intensity. This transition apparently does not originate in the ground state, and from the temperature-dependent intensity it can be concluded that the state in which the transition originates is situated some 5 cm^{-1} above the ground state. The energy difference between the ground state and this first excited state increases upon

TABLE III. The intensity of Raman lines of symmetry A_{1g}, E_g, T_{2g}, and T_{1g} as function of the angle φ.

$I_{A_{1g}}$	I_g	~	$\sin^2\varphi$		
	I_{Eg}	~	$3\cos^2\varphi$	+	$\sin^2\varphi$
	$I_{T_{2g}}$	~	$\cos^2\varphi$	+	$2\sin^2\varphi$
	$I_{T_{1g}}$	~	$2\cos^2\varphi$	+	$\sin^2\varphi$

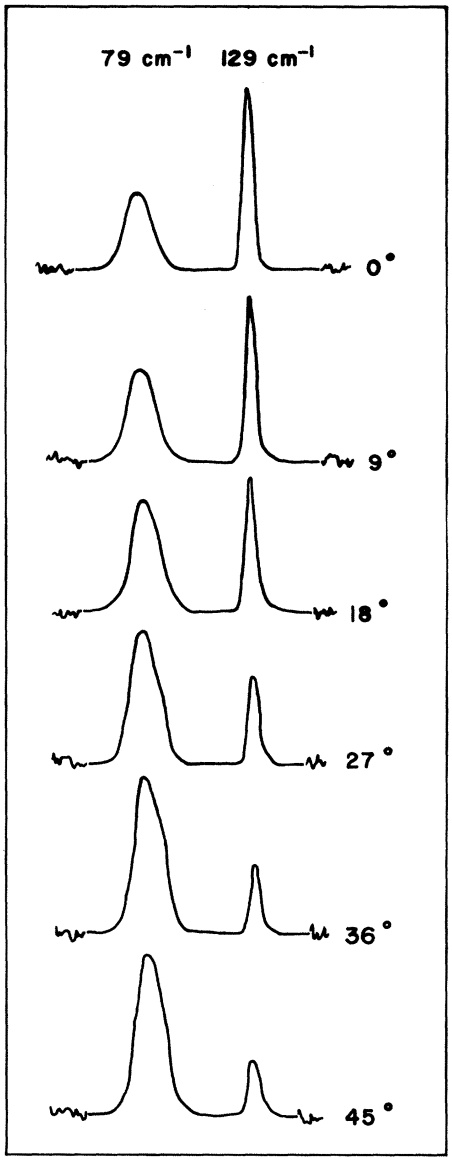

FIG. 2. Intensity of Raman bands of TbAlG centered at 75 cm^{-1} as function of the angle φ. Intensity dependence reveals that the transition is of symmetry T_{2g} (see also Table III).

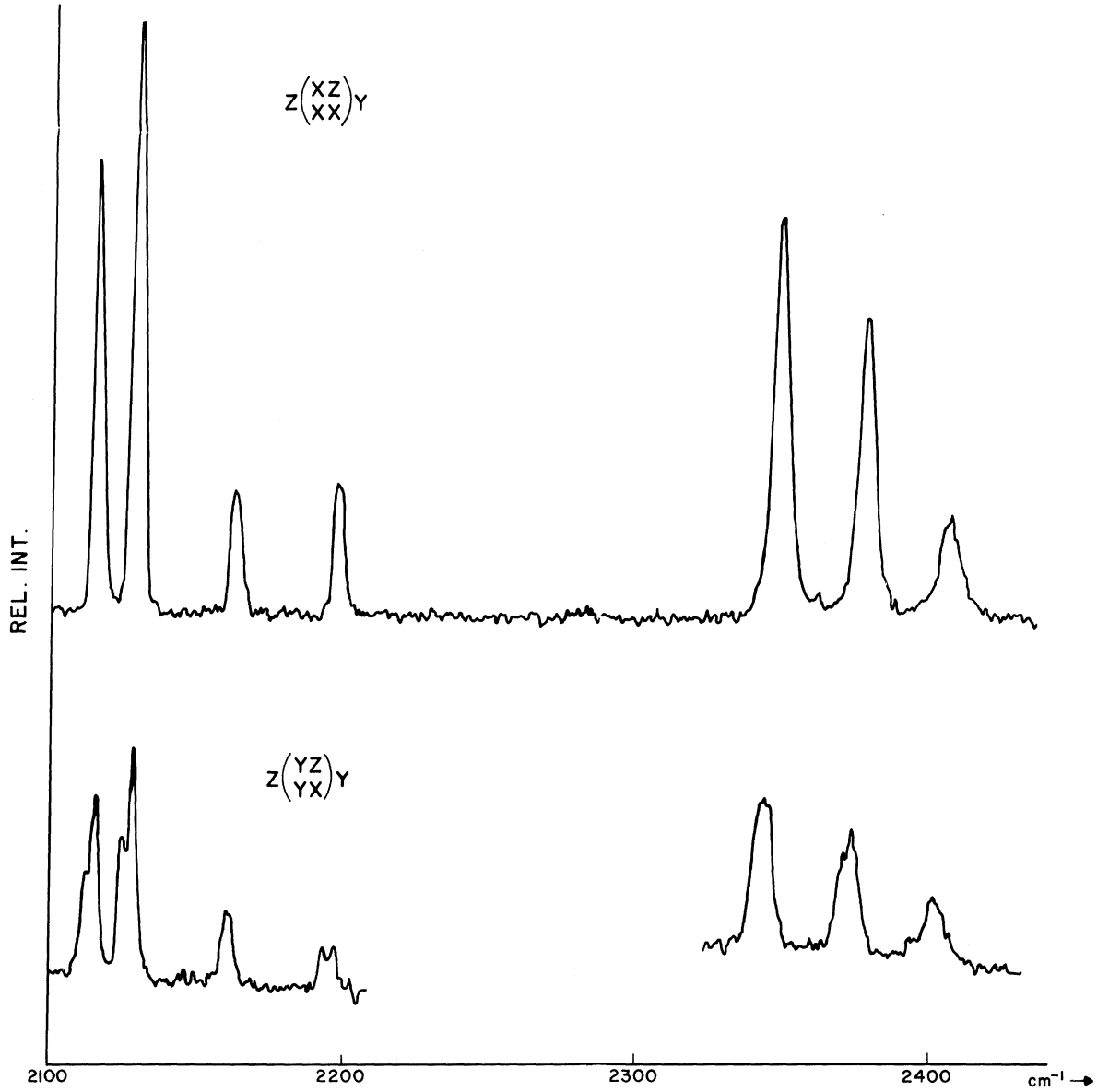

FIG. 3. $^7F_6$-$^7F_5$ electronic Raman transitions of TbAlG at 4.2 °K. $z\,(^{xz}_{xz})\,y$ stands for $z\,(xz)y + z\,(xx)\,y$, and the tensor elements are for the experimental case only. Tensors are given in Table II. Also shown are the transitions if the sample is exposed to an external applied magnetic field. Appearance of shoulders at the low-frequency side of the bands at lower-frequency shifts is due to the presence of an electronic state situated at ~ 5 cm^{-1}. See Fig. 5 and text for details.

exposing of the sample to strong magnetic fields. The population of the excited state decreases rapidly (the temperature of the sample is 4.2 °K) and the intensity of this excited-state transition (or hot band) decreases. It is seen that the intensity of the transition is negligibly small if the field reaches a value of 36 kG. Also the Raman transition centered around 74.6 cm^{-1} changes in frequency if the field becomes stronger. The energy-level diagram of Fig. 5 sums up the results of the Zeeman-Raman study.

The external applied magnetic field was parallel to the local z axis of two of the six sites for the terbium ion. Owing to the small splitting effects as compared with the experimental slit width, the splitting due to these two different directions of the magnetic field in the local axis system could not be observed. Splitting patterns due to the three different sites have been observed for some rare-earth garnet crystals employing ordinary tech-

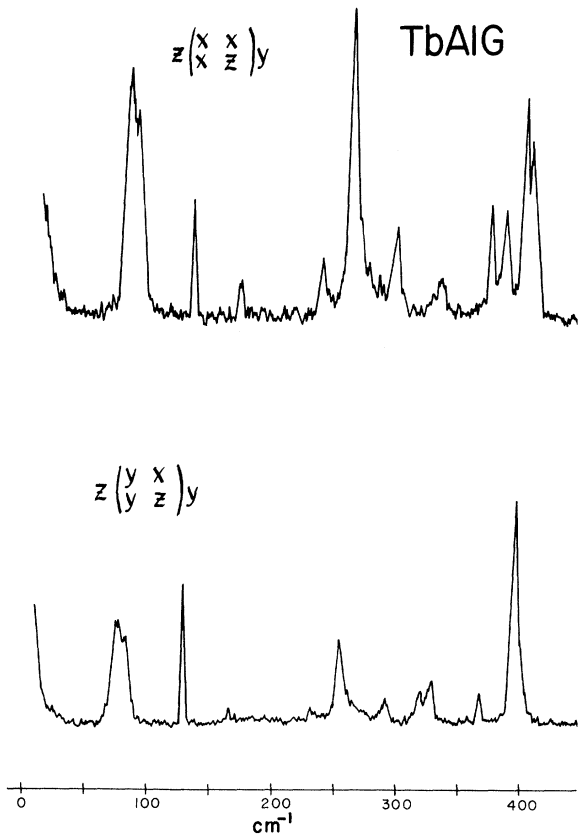

FIG. 4. Phonon and electronic Raman spectrum of TbAlG below 400 cm^{-1}. See Table IV for the position of electronic transitions.

niques of fluorescence or absorption spectroscopy[16] in magnetic fields and, compared to these data, the magnetic effects reported here are less suitable for interpretation. But similar to the results of YbGaG the Raman experiments in a magnetic field[11] are of importance to separate phonon transitions from electronic Raman effects.

Other electronic Raman transitions between the Stark levels of the $^7F_6$ manifold of TbAlG were found by comparison of the phonon spectrum of YAlG with the Raman spectrum of this compound. Evidence was found that electronic effects occur in the region of 260 to 290 cm^{-1}, but because of the presence of strong phonon Raman scattering, the exact positions of electronic levels cannot be given here. Positions and assignments are given in Table IV.

V. RELATION BETWEEN ELECTRONIC SCATTERING PROPERTIES IN SITE- AND FACTOR-GROUP SYMMETRY

In Sec. III, the states of the terbium ion have been analyzed in terms of the representations of the factor group O_h.[10] This procedure needs justification because it assumes the presence of some kind of interaction between the rare-earth ions. In the paramagnetic state of the crystal such interactions, e.g., magnetic dipole or electrostatic multipole interaction energies, are usually regarded as small if compared to thermal energies. This suggests that the correct way to interpret the electronic levels should be in terms of site-group symmetry. The scattering properties of the terbium ion in the various sites as compared to the scattering properties of the crystal is discussed below.

It is readily seen that the scattering properties of the rare-earth ions of the whole crystal are obtained by transforming the scattering tensors $(\alpha_{\rho\sigma})^s_{kn}$ of each of the ions in the different sites s to the coordinate system of the experimental arrangement. This can be done by employing the rotational matrices R_s and R_s^{-1}, followed by squaring of the individual tensor components of the sites and adding them. The scattering tensor of the crystal is then obtained in the following way:

$$[(\alpha_{\rho\sigma})_{kn}]^2_{\text{crystal}} = \sum_{\text{sites}} [R_s(\alpha_{\rho\sigma})^s_{kn} R_s^{-1}]^2 .$$

Although this procedure is straightforward, it is clear that interaction between the various lanthanide ions is not taken into account here. In fact, one might refer to the above as the case of incoherent scattering of the ions, which is in contrast to that of coherent scattering. The presence of some factor-group interaction is considered and the correlation of the different phases of the scattering centers of the six rare-earth sites is considered to be of importance.

TABLE IV. Frequencies and assignment of low-temperature Raman spectrum of TbAlG.

Raman shift (cm^{-1})	Symmetry of the transition of O_h	Symmetry of the excited state in D_2
0	···	B_1
~5	···	A
75	T_{2g}	B_2 or B_3
82*	T_{2g}	B_3 or B_2
262	A_{1g}	B_1
280–290	···	···
322	E_g	A
373	A_{1g}	B_1
2050*	E_g [A_{1g}, T_{2g}, T_{1g}]	
2071	E_g [T_{2g}, T_{1g}]	
2127	E_g [A_{1g}, T_{2g}]	B_1
2135	T_{2g}	B_3 or B_2
2148	T_{2g}	B_2 or B_3
2179	A_{1g}, E_g, T_{2g}	B_1
2210	T_{2g}	B_2 or B_3
2268*	[E_g]	
(2275)*	···	
2300	E_g	
2348	T_{2g}	B_3 or B_2
2376	T_{2g}	B_2 or B_3
2403	E_g [T_{1g}]	B_1
2463	[T_{2g}]	A
2485	[A_{1g}, E_g, T_{2g}, T_{1g}]	B_1

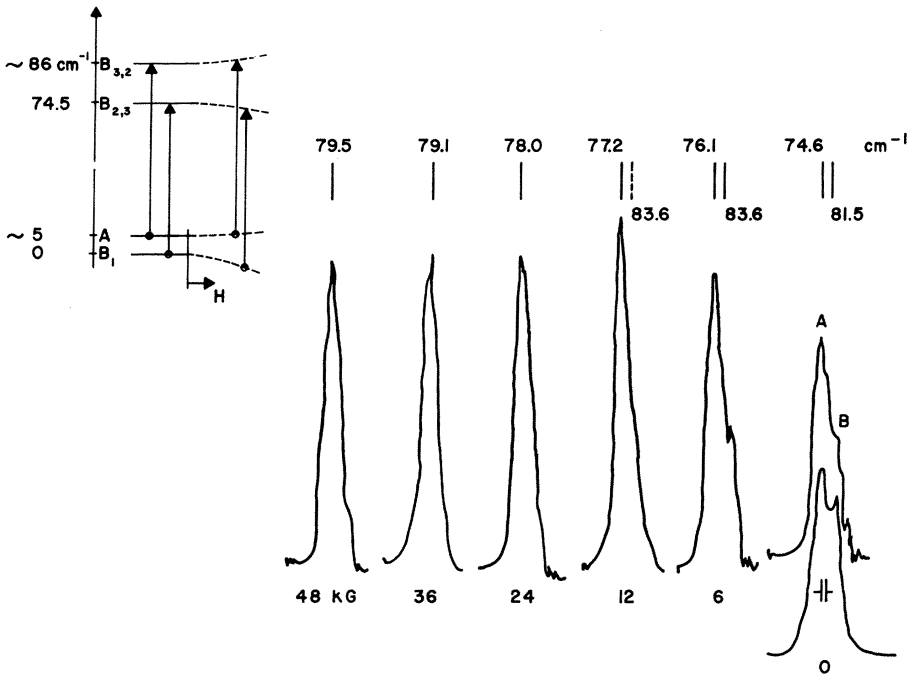

FIG. 5. The Zeeman-Raman results on electronic transitions of TbAlG, and part of the energy-level diagram.

Let H_0 be the Hamiltonian of the ion in the site symmetry and ϕ_{ks} its wave function in state k. H_i is the perturbing Hamiltonian describing the interionic energy. H_i transforms identically under the symmetry operations of the space group. The eigenfunctions Ψ_k of $H+H_i$ of the $k=0$ states, which are the only ones of importance and of interest in the first-order-type Raman process discussed here, belong to some of the irreducible representations of the factor group. These wave functions have in zeroth-order approximation the form

$$\Psi_k = (1/N)\sum_s A_{ks}\phi_{ks} .$$

The symbols have their usual significance except for A_{ks}. They are constants and chosen in such a way that the wave functions Ψ_k transform according to the representations of the factor group. Apparently, a determination of the A_{ks} is of paramount importance. For the case of the garnet crystals it is not necessary to have at hand a solution of a secular equation to find values of the constants.

From Table I it follows that the correlation of species of the site group D_2 to species of the factor group O_h is unique, in so far as the species of O_h occur only once. This permits the construction of the wave functions Ψ_k using symmetry arguments alone. If the irreducible representation γ is one dimensional, then A_{ks} is the character of γ belonging to the symmetry elements, which transforms site 1 into site s. In the case of a two- or three-dimensional representation the rules for construction of symmetry coordinates in molecular physics should be employed.[17]

Using the wave functions Ψ_k for calculating the components of the scattering tensor in the normal way (the integral $\langle \Psi_n | \alpha | \Psi_k \rangle \neq 0$), the tensor for the unit cell of the crystal can be computed by superposition of components of the tensors of the sites, while now also taking into account various phase factors. Also orientation of the local axes should be considered here and the relation for the Raman intensity is then given by the expression

$$[(\alpha_{\rho\sigma})_{kn}]^{-2}_{\text{crystal}} = [\sum_{\text{sites}} A^*_{ns} A_{ks} R_s (\alpha_{\rho\sigma})^s_{kn} R_s^{-1}]^2 .$$

The angles of rotation which are important for the matrices R_s and R_s^{-1} of the different sites are given in Table V and the results of the computation of a coherent tensor where the tensor elements transforming identically to the species of the totally symmetric representation of the group D_2 are considered is shown in Table VI.

TABLE V. Angles of rotation around the local axes, which relate the local coordinate systems to the system of the experiment (compare Fig. 1).

Site	φ_1	φ_2	φ_3
a	∘ ∘ ∘	∘ ∘ ∘	∘ ∘ ∘
b	(*z*); +90°	∘ ∘ ∘	∘ ∘ ∘
c	(*z*); +45°	(*x*); +90°	(*z*); +45°
d	(*z*); +45°	(*x*); +90°	(*z*); +45°
e	(*z*); + 45°	(*y*); − 90°	(*z*); +45°
f	(*z*); − 45°	(*y*); − 90°	(*z*); +45°

TABLE VI. Elements of the incoherent scattering tensor for the crystal originating from a diagonal tensor with a, b, c along the diagonal. This tensor has the transformation properties of the species A of the group D_2 and $A_{1g}+E_g+T_{2g}$ of O_h.

$4(a^2+b^2)$ $+(a+b+2c)^2$	$(2c-a-b)^2$	$2(a-b)^2$
$\frac{1}{4}(2c-a-b)^2$	$4(a^2+b^2)$ $+(a+b+2c)^2$	$2(a-b)^2$
$2(a-b)^2$	$2(a-b)^2$	$2c^2+4(a+b^2)$

For scattering tensors transforming under the species B_1, B_2, and B_3 of the group D_2 a similar procedure can be followed and the results of the calculations are summarized in Table VII. If there is no interaction between the ions of the different sites, or if the interaction is very weak then the factor-group splitting of the lines in the Raman spectrum is zero or not observable. The transitions with different symmetry occur at the same frequency. In the case of incoherent scattering the same result is obtained because the calculated scattering tensor (see Table VI) can be decomposed into components which have the same transformation properties as the species A_{1g}, E_g, and T_{2g}. There is no difference in comparing the case of the incoherent tensor with that of the coherent tensor except perhaps that for interpretation of the composition of individual elements of the total scattering tensor, the case of coherent tensor is more convenient. This is particularly true if the symmetry of the crystal field which the terbium ion experiences is related to polarization features of electronic Raman transition of the TbAlG crystal.

VI. PSEUDOTETRAGONAL CRYSTAL FIELD OF TERBIUM ALUMINUM GARNET

The results of computation of the elements of the coherent scattering tensor given in Table VII and experimental data of Table IV permit a unique determination of the symmetry of the crystal field which the terbium ion experiences in TbAlG. Although the site symmetry is orthorhombic, the question which remains to be answered is, does the crystal field deviate very strongly from tetragonal symmetry or is the actual field a pseudotetragonal field?[18-22]

When a rare-earth ion is placed in a surrounding of real tetragonal symmetry and the symmetry of the crystal is again cubic, coherent scattering tensors can again be constructed. For a tensor transforming identically according to the species A of the tetragonal group D_{4h}, the following is found, $a=b\neq c$ (compare Table VI), and the elements α_{xz} and α_{yz} of the coherent tensor are equal to zero. If, on the other hand, the actual symmetry at the site is orthorhombic, then $a\neq b\neq c$ and the above-mentioned elements of the tensor are not zero. The elements of tensor for the electronic Raman transition at 2179 cm^{-1} have been measured because this tensor is of symmetry $A_{1g}+E_g+T_{2g}$ and the transition connects electronic levels of symmetry B_1. From polarization measurements, the value $a/c=0.12\pm0.04$ is calculated and the Raman spectrum $Z(XZ)Y$ shows that this particular electronic transition has vanishing intensity, demonstrating that $a\approx b$. For the line at 2402 cm^{-1}, a value $a/c=0.08\pm0.04$ has been found. Again the XZ component of this transition has zero intensity.

For a field of tetragonal symmetry, some of the Stark components of the $^7F_5$ manifold are twofold degenerate. This degeneracy is removed if the field tends toward lower symmetry and, if the deviation remains small, the the splitting of the levels is also small. For the correlation, from Table VIII, it follows that the symmetry of these levels is either B_2 or B_3 in D_2. In order to find the proper scattering tensor to such states it is necessary to know the symmetry of the ground state. From an analysis of the transitions to the $^7F_5$ manifold levels only the symmetry B_1 of the ground state fits the experimental data, and the tensors for the transitions can thus be found. They are also given in Table VIII.

One particular feature of the $^7F_5$ transitions (see Fig. 4) is that the stronger transitions are of symmetry T_{2g}. They appear in pairs and close to these pairs is found a Raman line of symmetry $A_{1g}+E_g+T_{2g}$. The transitions of symmetry T_{2g} terminate in levels of symmetry B_2 or B_3 while other transitions terminate in a level of symmetry B_1. It is seen from Table VIII that these sets of levels can be thought of as being related to the species T_{1g} if the symmetry of the surrounding was cubic. The threefold degeneracy has, however, been removed, and the energy differences of the

TABLE VII. Elements of the symmetric scattering tensor computed for the case of the coherent scattering tensor in garnet crystals. The tensor in the site group is the same one as given in Table VI (A-type transition).

Species	Elements
A_{1g}	$xx=yy=zz=\frac{2}{3}(a+b+c)^2$; $xy=yz=zx=0$
$E_g^{(\alpha)}$	$xx=yy=\frac{1}{12}(a+b-2c)^2$; $zz=\frac{1}{2}(2c-a-b)^2$ $xy=yz=zx=0$
$E_g^{(\beta)}$	$xx=yy=zz=yz=zx=0$; $xy=\frac{1}{4}(2c-a-b)^2$
$T_{2g}^{(\alpha)}$	$xx=yy=\frac{1}{2}(a-b)^2$; $zz=xy=yz=zx=0$
$T_{2g}^{(\beta)}=T_{2g}^{(\alpha)}$	$xz=yz=\frac{1}{2}(b-a)^2$; $xx=yy=zz=xy=0$

TABLE VIII. Correlation of species of O_h, D_{4h}, and D_2 for the $J=5$ manifold. Also given is the symmetry of the various scattering tensors if the symmetry of the ground state is B_1 of D_2. For the $^7F_5$ manifold, the species T_{1g} occurs twice.

O_h	D_{4h}	D_2	Tensor (in D_2)
E_g	A_{1g}	A	B_1
	B_{1g}	B_1	A
T_{1g}	A_{2g}	B_1	A
	E_g	B_2	B_3
		B_3	B_2
T_{2g}	B_{2g}	A	B_1
	E_g	B_2	B_3
		B_3	B_2

Raman lines at 2135 and 2148 cm^{-1} and at 2348 and 2376 cm^{-1} suggest that the actual field which the terbium-ion experiences deviates from tetragonal symmetry[19]; but the deviation is apparently not very pronounced, in agreement with findings of measurement of the components of the tensor of the Raman transition (2179 and 2402 cm^{-1}).

An accurate measurement of symmetry properties of the Raman lines at 2348 and 2376 cm^{-1} reveals that these lines are not pure T_{2g} transitions. The polarization features suggest that species T_{1g}, representing the antisymmetric components of the scattering tensor, makes a contribution. The amount of antisymmetry could be determined by using relations between the different tensor components, which can be evaluated from Table II. Values for d/c of approximately 50% were computed. The contribution of antisymmetric tensors is, however, small compared to the total intensity of the $^7F_5$ transitions, and this is in good agreement with previously published data for this ion.[13]

VII. CONCLUDING REMARKS

In this paper the routine has been outlined that is necessary for the interpretation of the electronic Raman spectra of rare-earth garnet crystals. This is of special interest if positions and polarization properties of the electronic Raman transitions are connected with the results of crystal-field theory. It has been shown that symmetry of the crystal field can give rise to specific features in the scattering tensors.

The spectra shown in this paper were all excited with lasers with powers of up to 100 mW in the lines. The electronic Raman transitions were easily detectable but for exact measurement of polarization properties a stronger exciting source is necessary. We are planning to study the crystal in the near future with a stronger laser (700 mW) and the result of a Raman crystal-field calculation will be communicated in the next paper of this series.

ACKNOWLEDGMENT

The authors wish to thank Dr. L. G. Van Uitert of Bell Telephone Laboratories for supplying the terbium aluminum garnet crystal.

*Work supported in part by grants of the National Research Council of Canada and the Defense Research Board.

†Permanent address: Institut für Technische Physik, Technische Hochschule Darmstadt, Darmstadt, Germany.

[1]See, for instance, *Light Scattering Spectra of Solids*, edited by G. B. Wright (Springer-Verlag, New York, 1969), pp. 239–254.

[2]G. H. Dieke, *Spectra and Energy Levels of Rare-Earth Ions in Crystals* (Wiley, New York, 1968).

[3]J. Hougen and S. Singh, Phys. Rev. Letters 10, 406 (1963).

[4]J. A. Koningstein, J. Chem. Phys. 46, 2811 (1967).

[5]J. A. Koningstein and O. S. Mortensen, J. Opt. Soc. Am. 58, 1208 (1968).

[6]J. A. Koningstein, and O. S. Mortensen, Chem. Phys. Letters 2, 693 (1968).

[7]G. Menzer, Z. Krist. 69, 300 (1928).

[8]E. Prince, Acta Cryst. 10, 787 (1957).

[9]F. Euler and J. A. Bruce, Acta Cryst. 19, 971 (1965).

[10]J. A. Koningstein, Phys. Rev. 174, 477 (1968).

[11]J. A. Koningstein and G. Mace, Chem. Phys. Letters 3, 433 (1969).

[12]G. Mace, Toaning Ng, G. Schaack, and J. A. Koningstein, Z. Physik 230, 391 (1970).

[13]O. S. Mortensen and J. A. Koningstein, J. Chem. Phys. 48, 3971 (1968).

[14]A. Kiel and S. P. S. Porto, J. Mol. Spectry. 32, 458 (1969).

[15]J. A. Koningstein, Chem. Phys. Letters 2, 469 (1968).

[16]*Optical Properties of Ions in Crystals*, edited by H. M. Crosswhite and H. M. Moos (Interscience, New York, 1967), p. 22.

[17]E. B. Wilson, Jr., J. C. Decius, and P. C. Cross, *Molecular Vibrations* (McGraw-Hill, New York, 1955).

[18]R. Pappalardo and D. L. Wood, J. Chem. Phys. 33, 1734 (1960).

[19]J. A. Koningstein and J. E. Geustic, Phys. Rev. 135, A717 (1964).

[20]J. J. Pearson, G. F. Herrmann, K. A. Wickersheim, and R. A. Buchanan, Phys. Rev. 159, 251 (1967).

[21]P. Grunberg, S. Hüfner, E. Orlich, and J. Schmitt, Phys. Rev. 184, 285 (1969).

[22]There has been considerable discussion on this point in the literature. Initially, emphasis was placed on the crystal field being close to cubic or tetragonal (Ref. 19) but detailed studies revealed that the symmetry of the crystal field is orthorhombic (Ref. 20). The crystal-field parameters associated with tetragonal symmetry are, however, large (Refs. 20, 21).